# ARTICLES

## Mechanolysis of Glucose-Based Polysaccharides As Studied by Electron Spin Resonance[1]

**Masayuki Kuzuya,* Yukinori Yamauchi, and Shin-ichi Kondo**

*Laboratory of Pharmaceutical Physical Chemistry, Gifu Pharmaceutical University, 5-6-1, Mitahora-higashi, Gifu 502-8585, Japan*

*Received: October 29, 1998; In Final Form: June 1, 1999*

We report the detailed study of mechanically induced free radical (mechanoradical) formation of glucose-based polysaccharides such as cellulose and amylose based on electron spin resonance (ESR) on its comparison with plasma-induced radicals of polysaccharides. The observed ESR spectra of mechanically fractured samples by ball milling at room temperature have shown the multicomponent spectra, which differ in pattern from those of plasma-irradiated cellulose but are similar to those of plasma-irradiated amylose. The systematic computer simulations disclosed that the observed spectra of cellulose consist of three kinds of spectral components, an isotropic doublet (I) assigned to a hydroxylalkyl-type radical at $C_1$, an anisotropic doublet of doublets (II) assigned to an acylalkyl-type radical at $C_2$ and/or $C_3$ as discrete components, and a singlet spectrum (III) assigned to dangling-bond sites (DBS), while those of amylose consist of two kinds of spectral components, I and III. One of the most intriguing facts is that the component radicals are all glucose-derived mid-chain alkyl-type radicals as in the case of plasma irradiation, although it is known that mechanoradicals are produced by the polymer main-chain scission. It can be reasonably assumed, therefore, that the mechanoradicals primarily formed by 1,4-glucosidic bond cleavage of polysaccharides at room temperature underwent a hydrogen abstraction from the glucose units to give rise to the glucose-derived mid-chain alkyl-type radicals. Furthermore, spectrum III was a major component in the simulated spectra of both cellulose and amylose, unlike those in the case of plasma irradiation, suggesting that cross-linking reactions simultaneously occur accompanied by a decrease in the molecular weight in the course of vibratory milling.

### Introduction

The study of mechanolysis by the methods such as ball milling, pulverization, grinding, cutting, compression, and so on is of fundamental significance in connection with manufacturing a wide variety of solid materials in the entire field of industry. Polymers including polysaccharides in pulverized form are also very often used in a variety of industrial fields. It has been long known that mechanolysis of polymers, synthetic and natural, gives rise to mechanically induced radicals, so-called mechanoradicals, due to the polymer main-chain scission, when the mechanolysis is conducted at a temperature lower than the glass transition temperature ($T_g$) of the polymers.[2]

Since most operations of pulverization for a practical use are conducted at room temperature, we believe that the investigation of mechanolysis at room temperature can provide information useful for understanding not only the nature of mechanoradical formation but also the changes in physicochemical and mechanical properties in many polymers practically used, although such polymers studied will be limited to ones whose $T_g$ exceeds room temperature.

Most electron spin resonance (ESR) studies of mechanoradical formation reported previously dealt with polymers pulverized in liquid nitrogen (77 K), followed by temperature annealing,[3] and no systematic ESR study of mechanoradical formation at room temperature coupled with changes in the other physicochemical properties has been worked out other than several papers from our laboratory.[4]

Over the years a number of papers have dealt with the mechanical degradation of cellulose and its derivatives from various aspects due to their industrial importance.[5−8] Mechanochemical reactions of powdered cellulose, however, are composed of complicated processes involving not only the occurrence of the main-chain scission to give mechanoradicals followed by their ensuing reactions, including intra- and intersegmental recombination reactions,[5−7] but also the decrease in the molecular weight,[5] the disruption of crystallinity,[6,7] the particle size reduction,[7] and so on.[8]

Several authors have also reported the ESR studies on mechanoradical formation of cellulose including characterization of the mechanoradical structures,[5,9] but the ESR kinetics for mechanoradical formation has not been well investigated.

In view of the severe broadening of powder ESR spectra due to a small amount of anisotropy in the $g$ and/or α-hydrogen hyperfine tensor as well as the outlines of multicomponent spectra, as is usually observed with polymer radicals, an unambiguous identification of the powder radicals cannot generally be made on the basis of a single ESR spectroscopic

* Corresponding author. E-mail: kuzuya@gifu-pu.ac.jp. Fax +81-58-237-5979.

10.1021/jp984278d CCC: $18.00 
Published on Web 09/03/1999

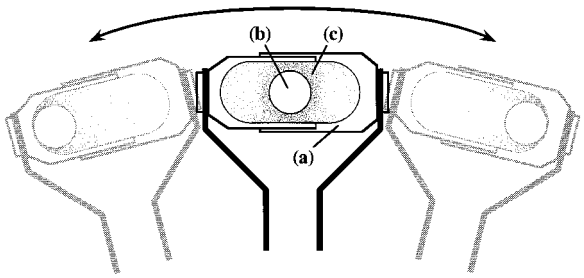


**Figure 1.** Illustration of vibratory ball milling used in the present work.

evidence alone, even if the computer-assisted deconvolution was conducted. Nevertheless, the direct analyses of the spectra could provide fruitful information about the nature of the mechanoradical formation, if one can carry out the systematic studies including the ESR kinetics coupled with the aid of computer simulations.

Thus, we have systematically conducted mechanolysis of cellulose and amylose at room temperature as representative examples of glucose-based polysaccharides, and the nature of mechanoradical formation including the kinetic analyses was studied by ESR with the aid of the systematic computer simulations.

In this paper, we report the full account of detailed analyses of the ESR spectra together with the kinetics for changes in the physicochemical properties in comparison with those of plasma-irradiated samples,[10] presenting novel and significant findings involved in mechanolysis of cellulose at room temperature.

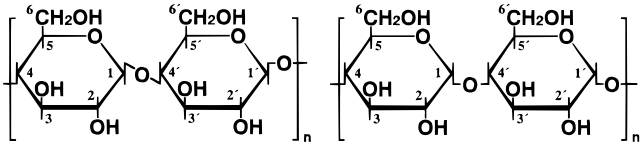


## Experimental Section

**Materials.** Microcrystalline cellulose ($T_g$ = 142.5 °C, $\bar{M}_w$ = ca. 53 200), commercially known as Avicel PH-102, and amylose ($T_g$ > 230 °C, $\bar{M}_w$ = ca. 15 100) were purchased from Asahi Chemical Co. Ltd., and from Kishida Chemical, respectively. Both polymer samples were screened with a 60−100 mesh sieve, and dried at 70 °C for 3 days in vacuo before use.

**Vibratory Milling.** A prescribed quantity (100 mg) of each polymer was mechanically fractured by a vibratory ball milling apparatus (Shimadzu Co. Ltd.) equipped with a stainless steel ball (6.0 mm ∅, 890 mg) in a stainless steel twin-shell blender (7.8 mm ∅, 24 mm long), or specially made Teflon ball (6.0 mm ∅, 290 mg) in a Teflon twin-shell blender (7.8 mm ∅, 24 mm long) (Figure 1), at room temperature for a prescribed period of time under anaerobic conditions in a vacuum glovebox (Samplatec Corp.). The frequency of vibratory ball milling was measured externally by use of a digital tachometer (model 3631, Yokogawa Co.). Air in the vacuum glovebox was replaced by purified nitrogen gas and then the remaining oxygen in this system was removed with a High Capacity Gas Purifier (Supelco, Inc.). The oxygen concentration was monitored with an oxygen analyzer (LC 750/PC-120, Toray Engineering Co. Ltd.) and kept below 0.01 ppm.

For ESR spectral measurement, each fractured sample thus obtained was transferred to a ESR sample tube and the tube was sealed in the vacuum glovebox.

**ESR Spectral Measurement.** ESR spectra were recorded by a JES-RE1X (JEOL) spectrometer with X-band and 100 kHz field modulation. Care was taken to ensure that no saturation occurred and that the line shape was not distorted by excessive modulation amplitude. From a plot of the square root of the microwave power versus the signal peak height, a microwave power level of 0.01 mW was chosen. The ESR spectral intensity was determined by double integration. The radical concentration (spin numbers per gram) was calculated from the spectral intensities with the aid of calibrated lines obtained from the spectral intensities of PMMA (poly(methyl methacrylate)) sample impregnated with DPPH. Measurements of $g$-values were made relative to the fourth signal from the lower magnetic field ($g$ = 1.981) of $Mn^{2+}$ in MgO.

**Computer Simulation of ESR Spectra.** Computer simulations were performed on a 32 bit microcomputer (NEC PC9821 Cx3). The simulated spectra were obtained from Lorentzian functions by fitting iteratively the spectroscopic parameters ($g$-value, line width at half-height, hyperfine splitting constant (HSC), and relative intensity) with the observed digitized spectra using a nonlinear least-squares method.[10,11] The simulation programs were fabricated so as to include the effect of anisotropy in the $g$-factor and/or α-hydrogen hyperfine tensor on the line shape of powder spectra according to Kneubühl's equation[12a] and Cochran's equation,[12b] respectively. An anisotropic interaction of $\beta$-hydrogens is usually small (less than 0.3 mT) so that such an effect is easily blurred due to broadening of the width of the individual peak and was not considered in the spectral simulation. To assist the simulation procedure, we have also fabricated the program for obtaining the difference spectrum by subtracting one observed spectrum from another.

**Molecular Weight Measurement.** The molecular weight of each fractured sample was measured by a gel permeation chromatograph (GPC; Shimadzu LC-6A), equipped with a refractive index detector (Shimadzu RID-6A), gel column (Shodex KD-800P and KD-80M), and a data analyzer (Shimadzu Chromatopac C-RA4), under the following conditions: elution solvent, dimethylacetamide containing 0.5% LiCl; flow rate, 0.7 mL/min; column temperature, 60 °C.[13] Calibration was carried out with a standard specimen of pullulan.

**X-ray Diffraction (XRD) Spectral Measurement.** The cellulose powder (ca. 180 mg) was placed in a sample holder and the surface was smoothed with a glass slide. Then, the crystallinity was measured by a powder X-ray diffraction meter (RAD-1C, Rigaku Co.) using Cu Kα radiation and a scan rate of 2 deg/min. The X-ray diffractograms were recorded between 5° and 40° in $2\theta$. The ratio of crystallinity in each spectrum was deduced by deconvolution of the spectra into sharp crystalline peaks and a halo pattern of amorphous regions with computer-assisted line fittings.

**Particle Size Measurement.** The mean particle size of each cellulose sample was measured by a laser scattering light analysis system (LDSA-2400A, Tohnichi Computer) using a dispersing-in-air-method at 3.0 kg/cm$^2$ of air pressure.

## Results

**Observed ESR Spectra of Fractured Cellulose and Amylose.** Figure 2 shows progressive changes in the room-temperature ESR spectra of cellulose and amylose mechanically

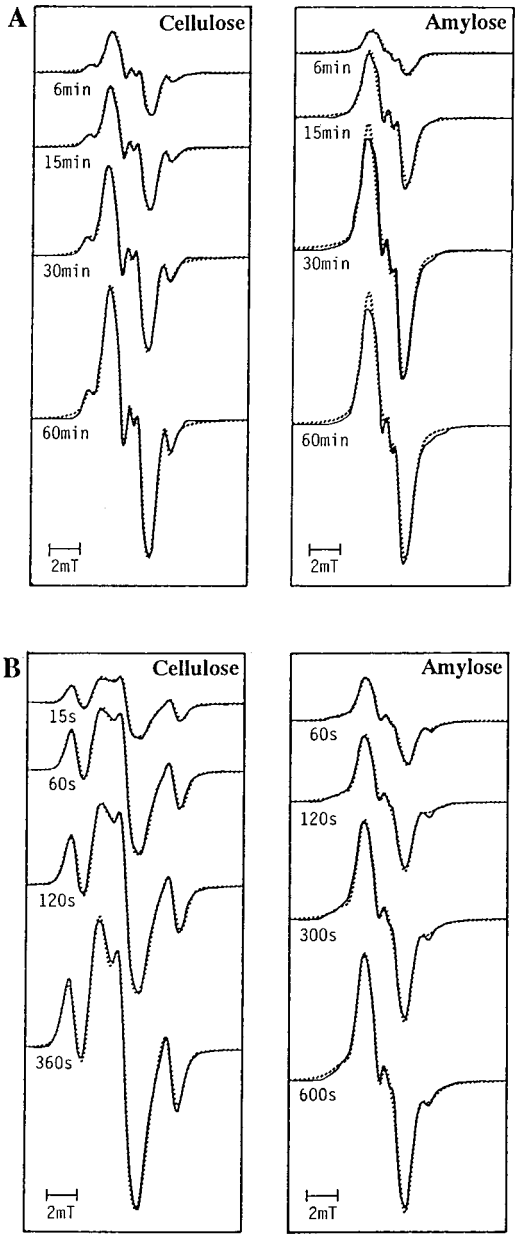


**Figure 2.** Progressive changes in observed ESR spectra of vibratory-milled cellulose and amylose (60 Hz vibration in $N_2$ at room temperature) (A) and argon plasma-irradiated cellulose and amylose (50 W irradiation power) (B), together with the simulated spectra shown as dotted lines.

fractured at 60 Hz vibration for various periods of time under anaerobic conditions (A) and of those plasma-irradiated for various durations for a comparison purpose (B),[10a] together with the corresponding simulated spectra shown as dotted lines.

It can be seen from Figure 2A,B that cellulose and amylose are appreciably different from each other in the spectral features, but the spectrum in each case remains nearly unchanged in the course of vibratory milling. And, the spectra of fractured cellulose are largely different from those of plasma-irradiated samples,[10a] although those of amylose are rather similar to each other.

When the respective sample fractured for 15 min, cellulose and amylose, was left to stand at room temperature under anaerobic conditions, the spectral pattern did not appreciably change even on prolonged standing in both cases, although all these spectra appear to be an outline of multicomponent spectra.

Figure 3 shows the progressive changes in the total spectral

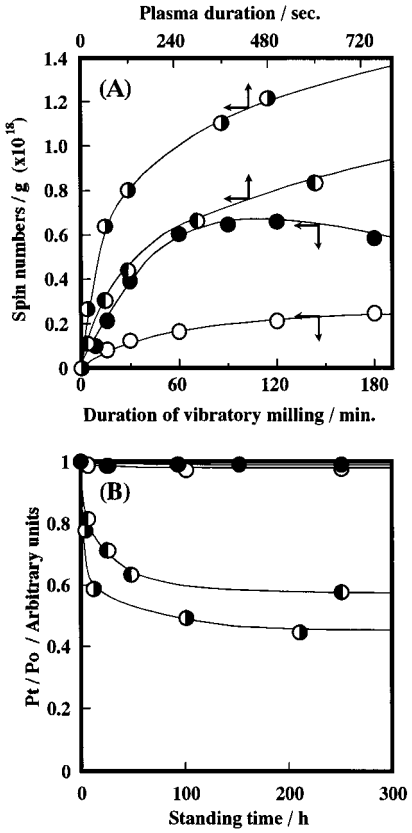


**Figure 3.** Progressive changes in spectral intensities determined by double integration: On vibratory milling of cellulose (●) and amylose (○), and plasma irradiation of cellulose (◑) and amylose (◐), and argon plasma irradiation (A). On standing anaerobically at room temperature of 15-min vibratory-milled and 180-s plasma-irradiated samples (B).

intensities as a function of duration of vibratory milling (A) and standing at room temperature (B), together with those by plasma irradiation.

It is seen from Figure 3A that the mechanoradical formation of both cellulose and amylose tends to level off at a much lower amount than that by plasma irradiation, and a longer vibratory milling of cellulose caused a decrease in the spectral intensity, which will be discussed later. Comparison in the progressive changes of the spectral intensity on standing at room temperature between mechanolysis and plasma irradiation clearly demonstrated that the mechanoradicals, unlike plasma-induced radicals, were quite stable for a long period of time at room temperature, indicating the absence of thermally unstable component radicals. However, when the sample was exposed to dry air at room temperature, the spectral pattern gradually changed in both cases toward a single broad line with a decrease in the total spectral intensity, as in the case of plasma-induced radicals, indicating the occurrence of reactions with oxygen to result in the formation of nonradical species.

It should be mentioned here that the spectral patterns of mechanoradicals were identical when amorphous cellulose or starch, instead of microcrystalline cellulose or amylose, were used for mechanolysis, although the spectral intensities varied somewhat with each other.

**Simulated Spectra.** We have systematically conducted computer simulations of these progressive changes in the complicated spectra in an interrelated manner. The simulated spectra corresponding to the observed spectra are shown in Figure 2 as dotted lines. It is clearly seen that all the observed spectra have been satisfactorily reproduced by the simulated spectra.

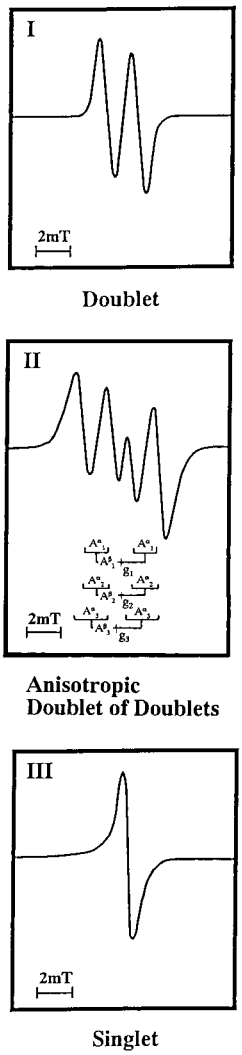


**Figure 4.** Three component spectra for the simulated ESR spectra.

**TABLE 1: ESR Spectral Data for Component Radicals in Simulated Spectra of Cellulose[a]**

| | I | II | | III | |
|---|---|---|---|---|---|
| $g$ | 2.0052 | $\bar{g} = 2.0045$ | $g_1 = 2.0040$ | $\bar{g} = 2.0046$ | $g_1 = 1.9996$ |
| | | | $g_2 = 2.0040$ | | $g_2 = 2.0068$ |
| | | | $g_3 = 2.0055$ | | $g_3 = 2.0074$ |
| $A\alpha$ | | $\bar{A}\alpha = 2.0045$ | $A_1 = 1.40$ | | |
| | | | $A_2 = 1.55$ | | |
| | | | $A_3 = 1.94$ | | |
| $A\beta(1)$ | 1.70 | $\bar{A}\beta = 2.94$ | $A_1 = 2.94$ | | |
| $A\beta(2)$ | - | | $A_2 = 2.94$ | | |
| | | | $A_3 = 2.94$ | | |

[a] Values of HSC are given in mT.

The computer simulations disclosed that there exist three component spectra in cellulose and two component spectra in amylose, all being essentially identical to those of plasma-irradiated amylose,[10a] and all the simulated spectra are obtained from admixtures of the component spectra with differing ratios. Figure 4 shows the representative spectral components of the simulated spectra of cellulose, one doublet (I), one anisotropic doublet of doublets (II), and a singlet spectrum (III). The simulated spectra of amylose were all obtained from I and III.

The ESR spectroscopic parameters for a representative selection of these component spectra of cellulose are summarized in Table 1, and those of amylose, in Table 2. The principal

**TABLE 2: ESR Spectral Data for Component Radicals in Simulated Spectra of Amylose[a]**

| | I | III | |
|---|---|---|---|
| $g$ | 2.0052 | $\bar{g} = 2.0047$ | $g_1 = 1.9999$ |
| | | | $g_2 = 2.0067$ |
| | | | $g_3 = 2.0074$ |
| $A\beta(1)$ | 1.70 | | |
| $A\beta(2)$ | - | | |

[a] Values of HSC are given in mT.

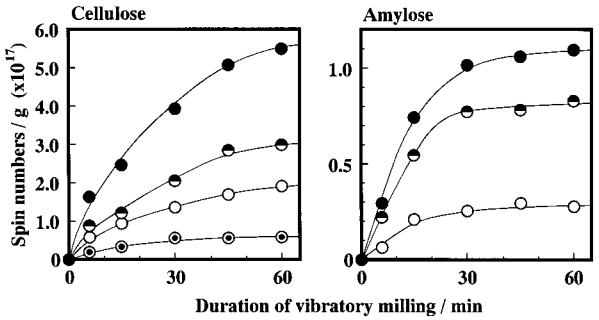


**Figure 5.** Progressive changes of spectral intensities of component spectra corresponding to the simulated spectra of cellulose (A) and amylose (B): (●) total; (○) **I**; (⊙) **II**; (◓) **III.**

anisotropic parameters vary somewhat with the spectra so that their values are only of semiquantitative significance.

Thus, a difference in the spectral pattern of fractured cellulose from that of plasma-irradiated cellulose is in the absence of the triplet component present in the plasma-irradiated cellulose. This is an essential reason the spectra of mechanolysis of cellulose appear to be different in pattern from those of plasma-irradiated cellulose.

The progressive changes in the spectral intensities of each component radical are shown in Figure 5. It is apparent that the ratio of each spectral intensity does not vary much with the time of vibratory milling, accounting for rather small spectral changes in pattern in the course of vibratory milling in both cases.

**Structural Assignments.** Simulated spectra in both cellulose and amylose are primarily characterized by the presence of a singlet spectrum (III) as a major component. Although the $g$-value of III indicated that it is a carbon-centered, not oxygen-centered, radical (ca. 2.0046 for cellulose and ca. 2.0047 for amylose), we cannot present any discrete radical structure for III. This radical may be a mixture of ring-opened and/or conjugated structures resulting from 1,4-glucosidic bond cleavages followed by its ensuing complex reactions and of no structural significance.

A nearly isotropic doublet (I) can be assigned to an alkoxylalkyl-type radical at $C_1$ (1) of the glucose unit formed by a hydrogen abstraction, as assigned in the case of various kinds of plasma-irradiated carbohydrates.[10,14] On the basis of the cosine square rule, the rather large $g$-value and smaller HSC for axial $\beta$-hydrogen at $C_2$ may stem from the influence of the two oxygens bonded to the radical center. And we can assign a doublet of doublets (II) with anisotropies in $g$-factor and $\alpha$-hydrogen hyperfine tensor to the acylalkyl-type radical at $C_2$ and/or $C_3$ (2), which has resulted from the facile dehydration of the hydroxylalkyl-type radical at $C_3$ and/or $C_2$ (Figure 6). The ESR spectrum cannot discriminate the alternatives.

## Discussion

**Nature of Mechanoradical Formation at Room Temperature on Its Comparison with That of Plasma-Induced**

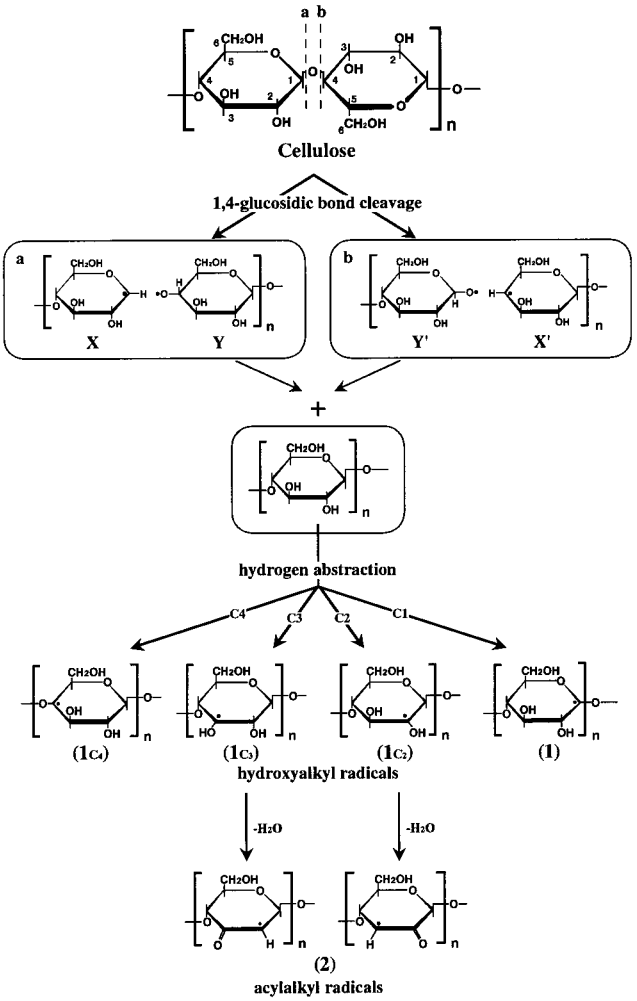


**Figure 6.** Structures of discrete mechanoradicals and the reaction sequence for its formation in cellulose.

**Surface Radicals.** One of the most intriguing findings in the present study is the fact that the observed mechanoradicals are all glucose-derived mid-chain alkyl-type radicals similar to those in plasma-irradiated cellulose and amylose, although it is known that the mechanoradicals are formed by polymer main-chain scission, i.e., 1,4-glucosidic bond cleavage. In fact, Hon et al. reported that 1,4-glucosidic bond cleavage occurred on mechanolysis of cellulose at 77 K, having observed one of the corresponding end-chain radicals by low-temperature ESR measurement.[5a] At the room-temperature mechanolysis, however, such end-chain radicals undergo the ensuing reaction to give the mid-chain alkyl-type radicals.

As shown in Figure 6 as a representative example, the 1,4-glucosidic bond scission of cellulose can formally give two pairs of end-chain radicals, two types of alkyl-type radicals, X and X′, and two alkoxy radicals, Y and Y′, and such end-chain type radicals may have rigorous molecular motion and high reactivities. Thus, such radicals could abstract a hydrogen atom at $C_{1-4}$ of the surrounding glucose units to give hydroxyalkyl-type radicals (1) and/or could undergo the radical−radical coupling to give nonradical species, accounting for the formation of the glucose-derived mid-chain radicals similar to those on plasma irradiation. It may be difficult otherwise to interpret the observed experimental facts. All these radical structures and reaction sequence are summarized in Figure 6.

To gain more insight, we have conducted several experiments to observe the mechanically induced radical-crossing reactions in various solid polymer combinations. The detailed result will be reported elsewhere, but the sense of the result is described here. The radical-containing *myo*-inositol plasma-irradiated for 3 min[14a] has submitted to a weak vibratory mixing using a Teflon vessel, under which no mechanoradical is formed, with virgin cellulose under anaerobic conditions. As a result, the cellulose-derived radicals were observed, the ESR spectra of the resulting mixture being similar to those of mechanoradicals discussed above. This demonstrates that hydrogens of cellulose were readily eliminated in contact with some other radicals in an intermolecular manner.

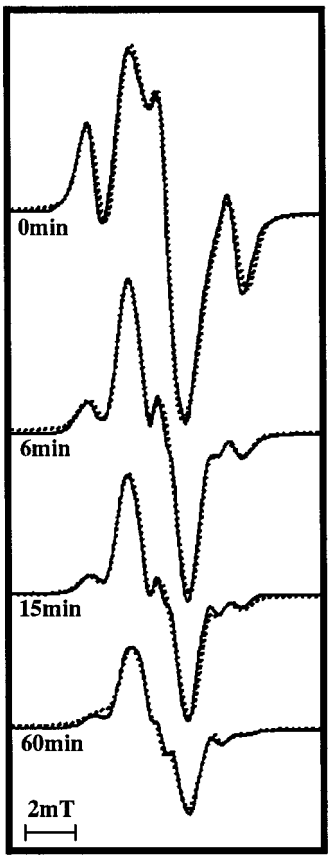


**Figure 7.** Progressive changes of ESR spectra of 180-s plasma-irradiated cellulose on vibratory mixing using a Teflon vessel.

Furthermore, another issue to be discussed is why a triplet spectrum with HSC of 2.98 mT assignable to hydroxyalkyl-type radicals of ($\mathbf{1}_{C_{2-4}}$)[10a] shown in Figure 6 was not observed in mechanolysis of cellulose but was observed in plasma irradiation. This anomaly has been understood by the following experiment. We have performed a weak vibratory mixing of Ar plasma-irradiated cellulose using a Teflon vessel. Figure 7 shows what happened to the ESR spectrum of plasma-irradiated cellulose, together with the simulated spectra shown as dotted lines.

It can be seen that the peaks of the triplet component quickly disappeared with a decrease in the total spectral intensity to convert into the spectra similar to that observed in the mechanolysis of cellulose (vide supra). The result indicated that, even if hydroxyalkyl-type radicals displaying a triplet spectrum are formed in the mechanolysis of cellulose, they should be dissipated during the course of vibratory milling due to the radical recombination reactions and/or occurrence of dehydration to acylalkyl-type radicals (2).

Furthermore, as shown in Figure 8, the spectral deconvolution based on the computer simulations disclosed that the other component spectra of a doublet (I) and a doublet of doublets

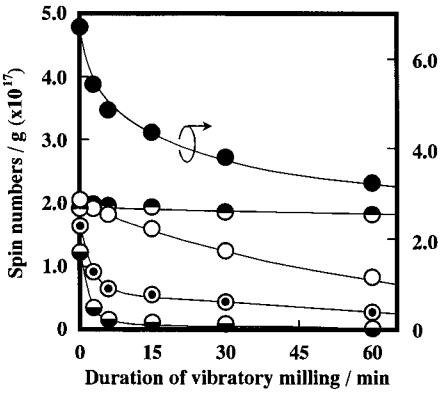


**Figure 8.** Progressive changes of component spectral intensities corresponding to the simulated spectra shown in Figure 7: (●) total; (○) doublet (I); (◒) triplet (with HEC of 2.98 mT); (⊙) anisotropic doublet of doublets (II); (◓) singlet (III).

(II) also appreciably decreased in intensity during the course of weak vibratory mixing. The result accounts concomitantly for the tendency of decrease in the spectral intensity of cellulose mechanically fractured at 60 Hz for a long period of time of vibratory milling, after reaching the limiting molecular weight (Figure 3).

Then, a question may arise as to why amylose lacks component spectrum II in the ESR spectra, unlike cellulose (vide supra). We note that the anomaly is apparently associated with the higher order structure of amylose, different from that of cellulose. If one does not consider the higher order structure of polymers, there is no obvious reason such a discrepancy in the radical formation has appeared between two anomeric polymers. Thus, a cylindrical projection (6−10 Å in cavity diameter) for tertiary structures of amylose clearly indicates that the axial hydrogens at $C_3$ in all α-glucose units of amylose are directed toward the inside of the spiral structure.[10a] The hydrogen abstraction at $C_3$ of amylose by the end-chain alkoxy radicals primarily forming the hydroxylalkyl radical, followed by dehydration resulting in the formation of the acyalkyl-type radical (2), would have been highly suppressed. On the other hand, cellulose is combined by a *β*-glucoside link to the $C_4$ hydroxyl group of another glucose unit and it is of linear structure. Therefore, such a restriction does not exist in cellulose.

**Concerning the Structural Diversity in Cellulosic Mechanoradicals on Its Comparison with Previous Works.** Cellulosic mechanoradicals have been studied with ESR in various phases by a number of investigators. However, the observed ESR spectra are often different in pattern from each other.[5−8] For example, Hon reported that the ESR spectra of mechanoradicals of cellulose produced from cotton fiber and/or wood cellulose during cutting and/or milling at ambient temperature and 77 K[5] and the ESR spectra observed by mechanical milling of cellulose are apparently different from the ones in the present work.[5c] It can be assumed that the reasons for this apparent contradiction could be due to a difference in the method of the mechanolysis, cutting, milling, or grinding and its strength and duration of mechanical force delivered as well as the nature of the cellulose samples used.

In addition, we would like to note several other possible reasons for such a discrepancy due to the method of ESR spectral measurement of the polymer samples. It is known that extra care should be taken for the modulation amplitude for the ESR spectral measurement of solid state radicals, especially saccharide radicals, since the line shape of the spectra would readily be distorted by the power saturation effect, let alone the measurement of low-temperature spectra (due to much lower molecular motion). Nevertheless, the ESR spectra were measured with a microwave power as large as 1−3 mW even at 77 K in several cases, while we have measured all the room temeperature ESR spectra with 0.01 mW.

Furthermore, the low-temperature ESR spectra have been measured for the sample being in liquid nitrogen (77 K).[5c] It is known, however, that any liquid nitrogen contains a trace of molecular oxygen, and most carbon-centered radicals are very sensitive to molecular oxygen. Thus, we have carefully monitored the amount of residual molecular oxygen in the reaction atmosphere, i.e., in nitrogen, and kept it always below 0.01 ppm throughout the experiments.

For the study of saccharide radicals, one should be further careful about this matter, since hydroxyalkyl-type radicals, one of the typical component radicals of saccharides, are well-known to undergo the dehydrogenation in contact with molecular oxygen to result in the formation of the ketones and hydroperoxy radicals (HOO•) without forming the corresponding peroxy radicals, as shown in[15]

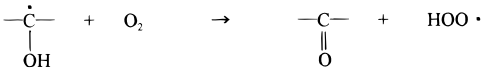


And the resulting hydroperoxy radicals can then be reacted with various sites of cellulose and may produce complex reactions. All these factors may also cause one to observe the ESR spectra previously appearing in the literature as different in pattern from ours.

It is also very difficult or even impossible to identify the powder radical structures on the basis of a single piece of ESR spectroscopic evidence alone without the aid of systematic simulations due to the severe broadening of individual peak width caused by a small amount of anisotropy in the *g* and/or α-hydrogen hyperfine tensor (vide supra). Many investigators, however, have attempted to present the mechanoradical structures based on a single piece of spectroscopic evidence, and subsequently the mechanism by which such radicals are formed varies with authors.

On the other hand, we have conducted systematic computer simulations of each observed time-course spectra of cellulosic mechanoradicals, with the aid of the result of various kinds of saccharide radicals, including *myo*-inositol, monosaccharides, and disaccharides, produced by argon plasmolysis, since the ESR spectra of mechanolysis of cellulose are similar in nature to the ones obtained by argon plasmolysis.

It is known that elimination of water from a hydroxyalkyl radical to give acylalkyl radicals is a characteristic reaction for saccharides,[16] and it was found from a series of systematic ESR studies on saccharide radicals that such reactions to give acylalkyl radicals also occur with the solid-state saccharides by argon plasmolysis.[14] In fact, since acylalkyl radicals have been formed as one of the component radicals in the room-temperature mechanolysis, such hydroxyalkyl radicals should have been formed from alkoxy radicals primarily generated by 1,4-glucosidic bond cleavage as described above, but under the present mechanical conditions, they readily underwent the dehydration reaction to give acylalkyl radicals effectively, as demonstrated by a separate experiment shown in Figure 7.

It was otherwise difficult to reproduce all the observed ESR spectra of cellulosic mechanoradicals by systematic computer simulations, including those of other saccharides and cellulose derivatives.

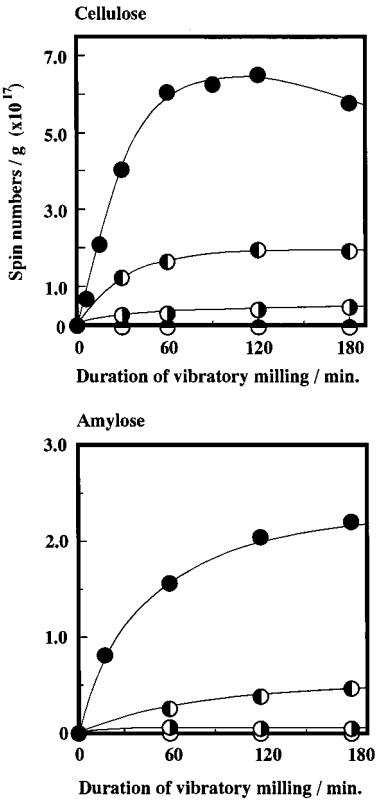


**Figure 9.** Progressive changes in ESR spectral intensities determined by double integration under various frequencies of vibratory milling of cellulose and amylose: (◓) 10 Hz; (◑) 20 Hz; (◐) 30 Hz; (●) 60 Hz.

**Systematic Analyses for Operational Factors Affecting Mechanoradical Formation.** To understand the nature of mechanoradical formation, we have further conducted kinetic studies on such a radical formation of cellulose under various mechanical conditions, monitoring the progressive changes of several physicochemical properties such as molecular weight, particle size, and crystallinity on a comparable basis.

Figure 9 shows the progressive changes in ESR spectral intensity of cellulose and amylose on their mechanolysis under various mechanical powers (represented by the frequency of a vibratory ball-milling), including 60 Hz vibratory milling, shown in Figure 3. It is seen that the mechanoradical formation increased as the mechanical power increased in both cases. It should be mentioned here that the ESR spectral pattern observed did not vary with mechanical power, weak or strong, which implies that the primary end-chain radicals formed by 1,4-glucosidic bond cleavage converted quite rapidly into the observed glucose-derived secondary mid-chain radicals.

The dependence of mechanoradical formation of cellulose on mechanical power was analyzed, and the mechanoradical formation at any given time of the earlier stage of vibratory milling (less than 60 min) was found to be linearly proportional to a square of frequency of vibratory milling, which can be written as $R_{mec} = A\omega^2$, where $R$ is spin numbers per gram ($\times 10^{17}$), $\omega$ is the frequency of ball-milling (Hz), and $A$ is a time-dependent proportionality constant comprising system-dependent parameters. Since $A$ represents the apparent rate of mechnoradical formation at any given frequency of a vibratory ball milling, $A$ was plotted against the time of milling ($t$), and the following relationship between $A$ and $t$ was obtained; $A = 2.29 \times 10^{14}(1 - e^{-0.0236t})$ ($r = 0.9977$).

Thus, using two operational parameters, $\omega$ and $t$, the mechanoradical formation of cellulose under the present method

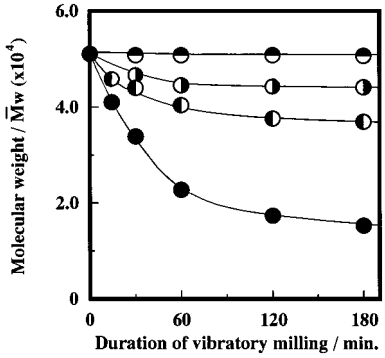


**Figure 10.** Progressive changes of molecular weight ($M_w$) of cellulose in the course of vibratory milling: (◓) 10 Hz; (◑) 20 Hz; (◐) 30 Hz; (●) 60 Hz.

can be eventually expressed as follows.

$$R_{mec} = 2.29 \times 10^{14}(1 - e^{-0.0236t})\omega^2 \quad (1)$$

The progressive changes of molecular weight ($\bar{M}_w$) in cellulose under various mechanical conditions were obtained from GPC measurements and shown in Figure 10. It can be seen that $\bar{M}_w$ of cellulose gradually decreased toward the corresponding limiting molecular weight ($\bar{M}_{w\infty}$) under various mechanical conditions. The more vigorous the mechanical condition is, the lower the $\bar{M}_{w\infty}$ is.

It is known in the case of vibratory milling of several kinds of polymers that the $\bar{M}_w$ decreased exponentially toward $\bar{M}_{w\infty}$, which has been expressed as follows:

$$\bar{M}_{wt} = \bar{M}_{w\infty} + (\bar{M}_{w0} - \bar{M}_{w\infty})e^{-kt}$$

where $\bar{M}_{wt}$ is a molecular weight at a given time of mechanolysis ($t$), $\bar{M}_{w0}$ is a molecular weight at $t = 0$, and $k$ is a proportionality constant comprising system-dependent parameters.[17]

In fact, each line of the progressive changes in $\bar{M}_w$ in Figure 10 was shown according to the above equation, proving that $\bar{M}_w$ of cellulose in the present method also exponentially decreased, from which the $\bar{M}_{w\infty}$ at each mechanical power has been deduced; $\bar{M}_{w\infty} = 44\,300$ for 20 Hz, $\bar{M}_{w\infty} = 37\,500$ for 30 Hz, $\bar{M}_{w\infty} = 15\,700$ for 60 Hz.

With a view to gaining more insight into the dependence of the decrease in $\bar{M}_w$ of cellulose ($\bar{M}_{w0} - \bar{M}_{wt}$) on mechanical power, such a decrease at a given time of an earlier stage of milling (less than 60 min) was plotted as a function of frequency and found to exhibit a linear line with respect to the frequency of vibratory milling, which can be written as $\bar{M}_{w0} - \bar{M}_{wt} = A\omega$. Then, each $A$ was plotted against the time of vibratory milling and the following relationship between $A$ and $t$ was obtained: $A = 589\ (1 - e^{-0.0272t})$ ($r = 0.9999$).

Thus, the decrease in the $\bar{M}_w$ of cellulose at an earlier stage of vibratory milling can be expressed as follows.

$$\bar{M}_{w0} - \bar{M}_{wt} = 589(1 - e^{-0.0272t})\omega \quad (2)$$

Comparison between two empirical equations, (1) and (2), indicates that the time course dependences are similar in nature to each other, but the mechanical power dependences are different from each other; i.e., the mechanoradical formation is proportional to $\bar{M}_{w0} - \bar{M}_{wt}$ (inversely proportional to $\bar{M}_{wt} - \bar{M}_{w\infty}$) but more sensitive than the change in $\bar{M}_{wt}$ with respect to mechanical power. This may be rationalized in terms of the fact that 1,4-glucosidic bond cleavage of cellulose caused by its mechanolysis directly corresponds to mechanoradical forma-

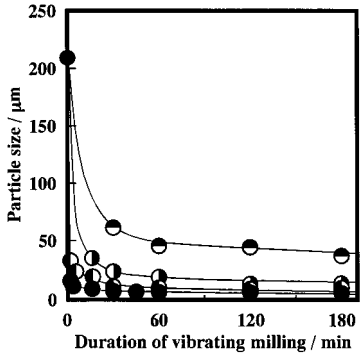


**Figure 11.** Progressive changes of the mean particle diameter of cellulose in the course of vibratory milling: (◓) 10 Hz; (◑) 20 Hz; (◐) 30 Hz; (●) 60 Hz.

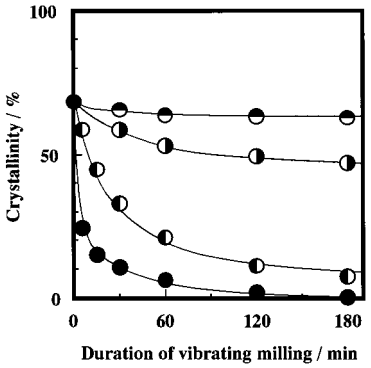


**Figure 12.** Progressive changes of the crystallinity of cellulose in the course of vibratory milling: (◓) 10 Hz; (◑) 20 Hz; (◐) 30 Hz; (●) 60 Hz.

tion, producing two types of primary end-chain radical centers, but $\bar{M}_w$ of polymers can be obtained only as an averaged degree of polymerization from the statistical analysis, so that observation of the change in $\bar{M}_{wt}$ should become less sensitive to the occurrence of a 1,4-glucosidic bond cleavage.

Figure 11 shows the results of progressive changes in mean particle size during the course of vibratory milling.

It is seen from Figure 11 that the particle size of cellulose was quite rapidly reduced to the limiting value under a given mechanical condition, including the weakest mechanical condition (10 Hz) presently examined, under which no mechanoradical formation was observed (Figure 9).

It is a well-known fact that particle size reduction in many kinds of powders is proportional to a cube of frequency of a ball milling in many vibration mills.[18] In fact, an examination of the relationship in cellulose between the particle size reduction and the frequency of vibratory milling using data at an earlier stage of vibratory milling has shown that it is proportional to a cube of the frequency at any given time of vibratory milling.

Finally, the progressive changes in crystallinity of cellulose deduced from the measurement of XRD spectra under various mechanical conditions are shown in Figure 12.

It is seen that the crystallinity quickly decreased and tends to level off at an earlier stage of the vibratory milling. For instance, the vibratory milling for 30 min at 60 Hz caused disruption of the crystallinity of cellulose from 68.7% to 12.0% (82.5% reduction), whereas, as is shown in Figure 9, the mechanoradical formation continues to occur even after 30 min of vibratory milling at 60 Hz.

It has been clearly demonstrated, therefore, that the reduction of particle size and disruption of crystallinity by vibratory milling should have essentially no bearing upon the mechanoradical formation.

## Conclusion

We have presented the nature of mechanoradical formation of two glucose-based polysaccharides, cellulose and amylose, based on the ESR spectral analyses coupled with systematic computer simulations and its comparison with that of plasma-induced radicals.

From the present study, the structures of mechanoradicals of cellulose and amylose were elucidated, which contain three component radicals for cellulose and two component radicals for amylose. A special feature is that a singlet spectrum (III) was a major component, assignable to the immobilized DBS (3) in both polymers, demonstrating that the room-temperature mechanolysis has a higher tendency to undergo the cross-link reaction.

The interesting contrast in the ESR spectra between plasma-induced radicals and mechanoradicals in cellulose is that the former spectra contain a large amount of isotropic triplets with 2.98 mT of HSC, while the latter spectra do not. As experimentally demonstrated, even if hydroxyalkyl-type radicals exhibiting such a triplet were formed, they are readily dissipated in the course of vibratory milling. The lack of the triplet in mechanolysis of cellulose is the essential reason for the difference in the spectral pattern from that of plasma irradiation.

One of the most intriguing facts is that the component radicals are all glucose-derived mid-chain alkyl-type radicals, as in the case of plasma irradiation, although a mechanistic study on a variety of polymers has firmly established that the mechanism by which the mechanoradicals are formed involves the polymer main-chain scission.[3,4,19] It has been confirmed that the mechanoradicals formed by 1,4-glucosidic bond cleavage of the polysaccharides at room temperature underwent hydrogen abstraction from the glucose units to give rise to the glucose-derived mid-chain alkyl-type radicals. Systematic analyses of physicochemical properties indicated that the mechanoradical formation is inversely proportional to the change in $\bar{M}_{wt}$ at any given mechanical power until $\bar{M}_w$ reaches the limiting value. It was also demonstrated that mechanical power has exerted an influence more sensitively on mechanoradical formation than the change in $M_{wt}$ of cellulose, although mean particle size reduction occurred in a much more sensitive manner with respect to mechanical power.

This type of result reported herein is not only of interest in its own right but also provides a basis for the future experimental criteria for preparation of a variety of powdered polysaccharides.

**Acknowledgment.** This work was financially supported in part by a Grant in Aid of Scientific Research from the Ministry of Education, Science, Sports, and Culture of Japan (Grant No. 09672191), which is gratefully acknowledged.

## References and Notes

(1) Part of this work was presented at 2nd International Symposium on Natural Polymers and Composites (ISNaPol 98), Atibaia-SP, Brazil, 1998.

(2) Haward, R. N. In *Amorphous Materials: Papers of the International Conference on Physics and Non-Crystalline Solids*, 3rd ed.; Douglas, R. W., Ellis, G., Eds.; John Wiley: London, 1970 (Pub. 1972); pp 513−521.

(3) Shoma, J.; Sakaguchi, M. *Adv. Polym. Sci.* **1976**, *20*, 109 and references cited therein.

(4) (a) Kuzuya, M.; Kondo, S.; Noguchi, A. *Macromolecules* **1991**, *24*, 4047. (b) Kuzuya, M.; Kondo, S.; Noguchi, A.; Noda, N. *J. Polym. Sci., Part A: Polym. Chem.* **1991**, *29*, 489. (c) Kuzuya, M.; Kondo, S.; Noguchi, A.; Noda, N. *J. Polym. Sci., Part B: Polym. Phys.* **1992**, *30*, 97.

(5) (a) Hon, D. N.-S. *J. Appl. Polym. Sci.*, **1979**, *23*, 1487. (b) Hon, D. N.-S.; Srinivasan, K. S. V. *J. Appl. Polym. Sci.* **1983**, *28*, 1. (c) Hon, D. N.-S. *Text. Res. J.* **1988**, *58*, 575.

(6) (a) Hess, K.; Kiessig, H.; Gundermann, J. *Z. Phys. Chem.* **1941**, *B49*, 64. (b) Hermans, P. H.; Weidinger, A. *J. Am. Chem. Soc.* **1946**, *68*, 2547. (c) Howsman, J. A.; Marchessault, R. H. *J. Appl. Polym. Sci.* **1959**, *1*, 313. (d) Leopold, B.; Moulik, S. K. R. *Tappi* **1968**, *51*, 334. (e) Caulfield, D. F.; Steffes, R. A. T*appi* **1969**, *52*, 1361. (f) Ikekawa, A.; Hayakawa, S. *Bull. Chem. Soc. Jpn.* **1983**, *56*, 3566. (g) BhamaIyer, P.; Sreenivasan, S.; Chidambareswaran, P. K.; Patil, N. B. *Textile Res. J.* **1984**, *54*, 732. (h) Otsuka, M.; Matsuda, Y. *Pharm. Technol. Jpn.* **1990**, *6*, 977. (i) Liang, X.-H.; Gu, L.-Z.; Ding, E.-Y. *Wood Sci. Technol.* **1993**, *27*, 461. (j) Wormald, P. *Cellulose* **1996**, *3*, 141.

(7) (a) Nakai, Y.; Fukuoka, E.; Nakajima, S.; Hasegawa, *J. Chem. Pharm. Bull.* **1977**, *25*, 96. (b) Nakai, Y.; Fukuoka, E.; Nakajima, S.; Yamamoto, K. *Chem. Pharm. Bull.* **1977**, *25*, 2490. (c) Nakai, Y.; Fukuoka, E.; Nakajima, S.; Yamamoto, K. *Chem. Pharm. Bull.* **1977**, *25*, 3340. (d) Nakai, Y.; Fukuoka, E.; Nakajima, S.; Iida, Y. *Chem. Pharm. Bull.* **1978**, *26*, 2983. (e) Nakai, Y.; Fukuoka, E.; Nakajima, S.; Yamamoto, K. *Chem. Pharm. Bull.* **1978**, *26*, 3419. (f) Nakai, Y.; Nakajima, S.; Yamamoto, K.; Terada, K.; Konno, T. *Chem. Pharm. Bull.* **1980**, *28*, 652.

(8) Ikekawa, A.; Hayakawa, S. *Bull. Chem. Soc. Jpn.* **1982**, *55*, 1261.

(9) (a) Hon, D. N.-S. *J. Polym. Sci., Polym. Chem. Ed.* **1980**, *18*, 1857. (b) Hon, D. N.-S. *Dev. Polym. Degrad.* 1**987**, *7*, 165.

(10) (a) Kuzuya, M.; Morisaki, K.; Niwa, J.; Yamauchi, Y.; Xu, K. *J. Phys. Chem.* **1994**, *98*, 11301. (b) Kuzuya, M.; Yamauchi, Y.; Niwa, J.; Kondo, S.; Sakai, Y. *Chem. Pharm. Bull.* **1995**, *43*, 2037.

(11) (a) Kuzuya, M.; Noguchi, A.; Ishikawa, M.; Koide, A.; Sawada, K.; Ito, A.; Noda, N. *J. Phys. Chem.* **1991**, *95*, 2398. (b) Kuzuya, M.; Ito, H.; Kondo, S.; Noda, N.; Noguchi, A. *Macromolecules* **1991**, *24*, 6612. (c) Kuzuya, M.; Niwa, J.; Ito, H. *Macromolecules* **1993**, *26*, 1990. (d) Kuzuya, M.; Yamashiro, T.; Kondo, S.; Sugito, M.; Mouri, M. *Macromolecules* **1998**, *31*, 3225. (e) Kuzuya, M.; Kondo, S.; Sugito, M.; Yamashiro, T. *Macromolecules* **1998**, *31*, 3230.

(12) (a) Kneubühl, F. K. *J. Chem. Phys.* **1960**, *33*, 1074. (b) Cochran, E. L.; Adrian, F. J.; Bowers, V. A. *J. Chem. Phys.* **1961**, *34*, 1161.

(13) Timpa, J. D. *J. Agric. Food Chem.* **1991**, *39*, 270.

(14) (a) Kuzuya, M.; Noda, N.; Kondo, S.; Washino, K.; Noguchi, A. *J. Am. Chem. Soc.* **1992**, *114*, 6505. (b) Kuzuya, M.; Yamauchi, Y.; Niwa, J.; Kondo, S. *Proc. Jpn. Symp. Plasma Chem.* **1996**, *9*, 55. (c) Kuzuya, M.; Yamauchi, Y. *Thin Solid Films* **1998**, *316*, 158. (d) Yamauchi, Y.; Sugito, M.; Kuzuya, M. *Chem. Pharm. Bull.* **1999**, *47*, 273

(15) (a) Carter, W. P. L.; Darnall, K. R.; Graham, R. A.; Winer, A. M.; Pitts, J. N. Jr. *J. Phys. Chem.* **1979**, *83*, 2305. (b) Ohta, T.; Bandow, H.; Akimoto, H. *Int. J. Chem. Kinet.* **1982**, *14*, 173. (c) Washida, N. *J. Chem. Phys.* **1981**, *75*, 2715. (d) Washida, N. *Bull. Chem. Soc. Jpn.* **1987**, *60*, 3757. (e) Miyoshi, A.; Matsui, H.; Washida, N. *J. Phys. Chem.* **1990**, *94*, 3016

(16) von Sonntag, C. *Adv. Carbohydr. Chem. Biochem.* **1980**, *37*, 7.

(17) (a) Harrington, R. E.; Zimm, B. H. *J. Phys. Chem.* **1965**, *69*, 161. (b) Kanamaru, K. *Kolloid-Z. Z. Polym.* **1966**, *209*, 151.

(18) (a) Rose, H. E.; Sullivan, R. M. E. *Vibration Milling and Vibration Mill*; Constable and Co.: London, 1961; pp 65−72. (b) Tamura. K.; Tanaka, T. *Ind. Eng. Chem. Process Des. Dev.* **1970**, *9*, 165.

(19) (a) Pilar, J.; Ulbert, K. *J. Polym. Sci., Polym. Phys. Ed.* **1978**, *16*, 1973. (b) Tabata, M.; Yamakawa, H.; Takahashi, K.; Sohma, J. *Polym. Degrad. Stab.* **1979**, *1*, 57. (c) Yamakawa, H.; Sakaguchi, M.; Sohma, J. *Rep. Prog. Polym. Phys. Jpn.* **1976**, *19*, 477.